Supplementary Information (SI) for Green Chemistry.
This journal is © The Royal Society of Chemistry 2024

Supporting Information

Postliminary treatment of food waste digestate via combined hydrothermal carbonization and microbial fuel cell for bio-energy recovery: A comparative life cycle impact assessment

Shraddha Yadav[a], Manikanta M. Doki[b], Makarand M. Ghangrekar [a,b,c]*, Brajesh Dubey[b]

[a] School of Environmental Science and Engineering, Indian Institute of Technology, Kharagpur, 721302, West Bengal, India

[b] Civil Engineering Department, Indian Institute of Technology, Kharagpur, 721302, West Bengal, India

[c] National Institute of Technology Puducherry, Karaikal, 609609, India

*Corresponding author: ghangrekar@civil.iitkgp.ac.in

Materials and Methods

Feedstock collection

Raw food waste (FW) was sourced from various locations within the Indian Institute of Technology, Kharagpur, including residential hostels, fruit and vegetable markets, juice centres, and residential quarters. The collected waste included rotten fruits (such as apples, oranges, bananas, and Indian jujube), vegetables (potato, brinjal, cauliflower, onion, ginger, garlic, etc.), peels, and leaves (from potato, carrot, cauliflower, cucumber, coriander, onion, etc.), along with sugarcane bagasse. This segregated FW underwent grinding to achieve uniform size for subsequent conversion into slurry, which was refrigerated (– 4 °C) until introduction into the reactor. A 10% inclusion of sugarcane bagasse slurry was implemented to assess the impact of feedstock heterogeneity. Later, the mixed slurry was utilized to analyse the biochemical methane potential.

Biochemical methane potential test

The assessment of biochemical methane potential (BMP) involved employing 2 L batch-mode reactors operating under mesophilic conditions within the temperature range of 32 ℃ – 37 ℃ for a 60-day duration (Fig. S1 a). Reactor vessels were charged with a 50:50 volume ratio of FW slurry and up-flow anaerobic sludge blanket reactor (UASBR) sludge, reaching a working volume of 1.6 L. After a nitrogen purging, the sealed reactor bottles were linked to the NaOH displacement tank, and the biomethane yield was determined by the volume of displaced solution due to produced biomethane [1]. To prevent the establishment of stagnant zones, manual stirring of the reactors was performed twice daily. Periodic pH adjustments were made every 15 days during the experiment to uphold optimal conditions for anaerobic digestion[2].

Hydrothermal carbonization of anaerobic digestate derived from food waste (AD-FW)

Hydrothermal carbonization (HTC) of AD-FW was conducted in a 50 mL Teflon-lined autoclave (Fig. S1 b) over a temperature range of 180 °C – 240 °C (increment of 30 °C) with residence times of 2 h, 4 h, and 6 h (selected as per the previous investigation conducted by Wang et al.)[3]. Sufficient moisture content in the digestate obviated the need for additional externally supplied water. The reactor was heated to the specified temperature and duration using a muffle furnace. After the designated residence time, the reactor was promptly immersed in an ice-water bath to arrest further reactions. Subsequently, the hydrochar (HC; solid fraction) was isolated via Whatman filter grade 42 and subjected to oven drying at 85 °C for 24 h to eliminate any volatile compound losses. The dried samples were securely stored in zip-lock bags for subsequent analyses. The resulting liquid phase (process water), termed HTC-PW, was preserved at a temperature of 4 °C for subsequent analysis.

Analytical characterization of hydrochar

Proximate analysis of AD-FW and HC, including moisture content, volatile solids (VS), and ash content, were performed as per standard protocols of American Society of Testing and

Materials (ASTM)-E871, ASTM-E1755, and ASTM-E872 [4–6]. Fixed carbon (FC) content was measured using the subtraction method (100 – Ash% – VS%). The percentage of carbon (%C), hydrogen (%H), nitrogen (%N), and sulphur (%S) in the composition of samples were conducted using an elemental analyser (EURO EA) in triplicates. The oxygen (%O) content was determined by the difference method following the Eq. (1). Thermogravimetric analysis (TG), i.e., temperature-based combustion experiment, was conducted using Perkin Elmer Pyris Diamond (TG- differential thermal analysis (DTA)) instrument within the range of 50 – 950 °C, controlled heating rate of 10 °C/min, and air flow rate of 100 mL/min. The key parameters, i.e., ignition temperature (T_i), burnout temperature (T_f), and maximum weight loss rate (T_m) were evaluated using the tangent intersection method. Additionally, the maximum weight loss rate (DTG_{max}) and average weight loss rate (DTG_{avg}) were also determined for evaluating combustion performance.

$$\%O = 100 - (\%C + \%H + \%N + \%S) \quad \text{(Eq. 1)}$$

To determine the morphology including the micro or macro structure inherent in hydrochar samples, the scanning electron microscopy analysis (SEM; MERLIN, Zeiss, Oberkochen, Germany) was performed. Further, the SEM-Energy Dispersive X-Ray (EDX) elemental mapping was conducted to identify the elements present in the HC. Fourier transform infrared spectroscopy (FTIR; FTIR spectrometer; Nicolet 6700; Thermo Fisher Scientific) was used to illustrate the surface functionality; whereas X-ray diffraction (XRD) patterns using X-ray diffractometer (Bruker D2 PHASER; Cu Kα radiation, λ = 0.15418 nm, scan angle range 2θ = 10−90°)) was used to observe crystalline phases of the HC samples [3]. Further, the organic content of HTC-PW in terms of total organic carbon (TOC; Shimadzu TOC-5000 analyser, Japan) was determined using the TOC analyser. The chemical oxygen demand (COD) was determined through the closed reflux spectrophotometric method of potassium dichromate after 24 h retention time [7].

Fuel characteristics of hydrochar

The HHV (MJ/kg) of the hydrochar sample was calculated employing Dulong's formula (Eq. 2) based on the elemental composition [8]. The HCY in terms of percentage of AD-FW feedstock was calculated using Eq. 3. Further, the energy performance of HC was evaluated by determining the fuel ratio (FR), energy densification (ED), and energy recovery efficiency (ERE %) using Eq. 4 – Eq. 6 [9].

$$HHV = 0.3383 \times \%C + 1.422 \times \left(\%H - \%\frac{O}{8}\right) \quad \text{(Eq. 2)}$$

$$HCY\ (\%) = \frac{dry\ mass\ of\ HC}{dry\ mass\ of\ anaerobic\ digestate} \times 100 \quad \text{(Eq. 3)}$$

$$Fuel\ ratio\ = \frac{Fixed\ carbon}{Volatile\ matter} \quad \text{(Eq. 4)}$$

$$Energy\ densification = \frac{HHV\ of\ hydrochar}{HHV\ of\ feedstock} \quad \text{(Eq. 5)}$$

$$Energy\ recovery\ efficiency\ (\%) = HC\ yield\ \times Energy\ densification \quad \text{(Eq. 6)}$$

Microbial fuel cell setup, polarisation, and metagenomic analysis

A laboratory-scale composite (clay with 20% montmorillonite) ceramic MFCs was used with an effective anolyte volume of 100 mL (Fig. S1 c). The monolithic composite ceramic had a thickness of 5 mm, which acts as a proton exchange membrane. The exterior wall of the ceramic composite was coated with a concoction prepared with polydimethylsiloxane (6.67 µL/mg of catalyst) and 0.5 mg/cm^2 carbon black. Both anode (surface area of 132 cm^2) and cathode (surface area of 194 cm^2) were fabricated using carbon-felt embedded with stainless steel wiring. Further, the electrodes were connected externally with a 100 Ω resistor to complete the

electric circuit. The whole assembly was placed in a plastic container with tap water as the catholyte with a provision of external continuous aeration.

The MFC was inoculated with anaerobic sludge (10% by volume) collected from the UASBR located at IIT Kharagpur, West Bengal, India. The inoculum was given pre-treatment with chloroform to suppress methanogens in the anodic biofilm [10]. Further, the anodic chamber was fed with HTC-PW having COD of 6000 mg/L (diluted with STP effluent in the ratio of 1:2) in batch mode of 72 h, respectively. The COD reduction was observed each day to analyse the organic matter degradation efficiency of the MFC.

Real-time voltage response in terms of the open-circuit voltage and operating voltage data was logged using an Agilent 30970A system (Agilent Technologies, Inc., Malaysia). The polarization profile was created by altering the external load with a variable-resistance in the range of 10 Ω – 20k Ω (Decade, India). The power generated was determined by multiplying the voltage (V) by the current generated (I) against the external resistance (R). The internal resistance of the MFC was estimated from the slope of the polarization curve, while the maximum power density was determined from the plot of power density against current density.

For 16s metagenomic analysis of the anodic biofilm, the amplification, and purification of the amplicons from the sample were conducted using Ampure beads to eliminate any residual primers [11]. Subsequently, an additional eight cycles of polymerase chain reactions were carried out employing Illumina barcoded adapters to facilitate the preparation of sequencing libraries. These libraries underwent purification once again using Ampure beads and were quantified utilizing the Qubit dsDNA High Sensitivity assay kit. Sequencing was executed utilizing the Illumina Miseq platform equipped with a 2x300PE v3-v4 sequencing kit. The above test was

conducted to identify the genes of exoelectrogens present in the anodic biofilm that contribute to electricity generation in MFC [11].

Life cycle assessment

The life cycle inventory (LCI) values in this investigation were derived from experimental studies conducted at IIT Kharagpur. For the present investigation, the functional unit of inventory was 1 kg of FW. Further, the eastern India electricity power mix was utilized for energy consumption. Environmental impacts were estimated by entering input and output data into SimaPro Version 8.0.3 LCA software. The Ecoinvent database provided the material and energy flow data for upstream and downstream processes. The impact assessment covered eighteen mid-point impact categories and four end-point damage assessment categories. Environmental impacts of all three systems were analysed by converting the calculated LCIs into corresponding environmental impact categories using the IMPACT 2002+® method (Swiss Federal Institute of Technology Lausanne, Switzerland) within SimaPro 8.0.3 [12]. The fifteen mid-point impact categories assessed were: (i) Global warming, (ii) Stratospheric ozone depletion, (iii) Ionizing radiation, (iv) Ozone formation, Human health, (v) Fine particulate matter formation, (vi) Ozone formation, Terrestrial ecosystems, (vii) Terrestrial acidification, (viii) Freshwater eutrophication, (ix) Marine eutrophication, (x) Terrestrial ecotoxicity, (xi) Freshwater ecotoxicity, (xii) Marine ecotoxicity, (xiii) Human carcinogenic toxicity, (xiv) Human non-carcinogenic toxicity, (xv) Land use, (xvi) Mineral resource scarcity, (xvii) Fossil resource scarcity, and (xviii) Water consumption. Additionally, three end-point damage assessment categories were evaluated based on a single score using the same dataset: (i) Human health, (ii) Ecosystem quality, and (iii) Resource recovery. The boundaries for the three systems S1 = AD, S2 = AD+HTC, and S3 = AD+HTC+MFC are stipulated in Fig S4.

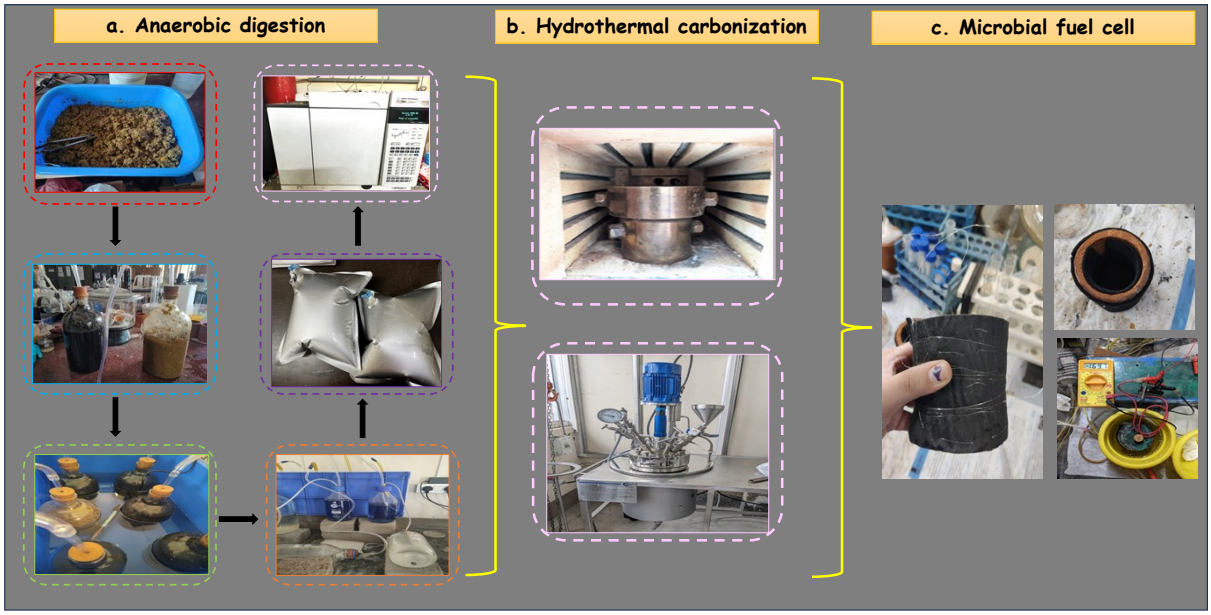

Fig. S1. Experimental set-up of **(a)** AD, **(b)** HTC, and **(c)** MFC

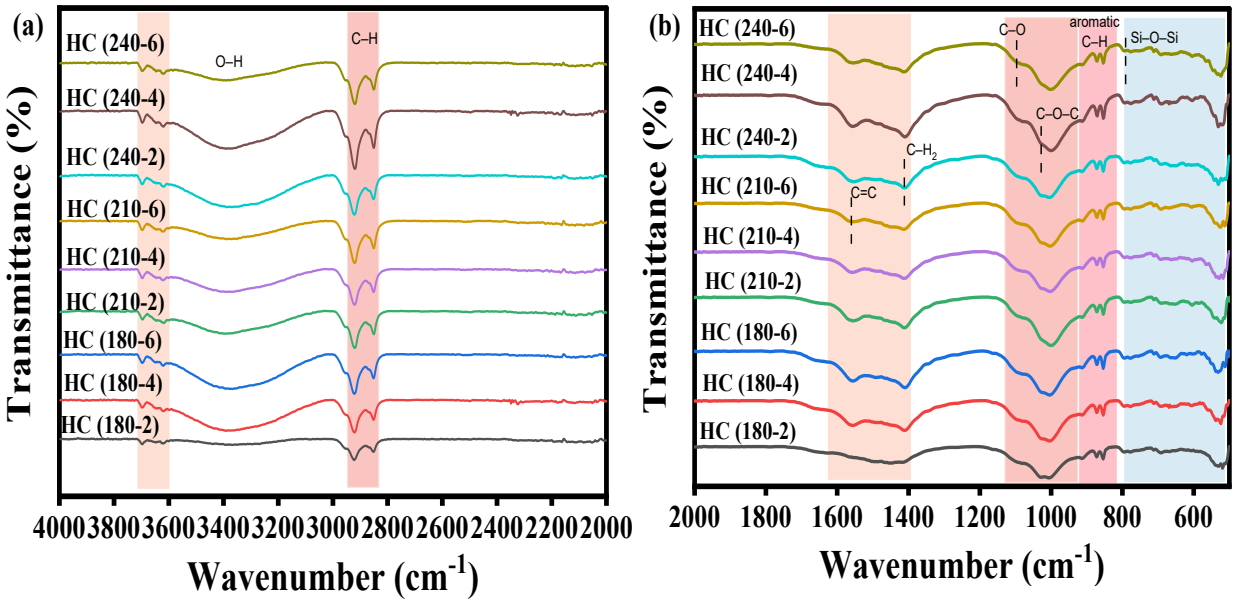

Fig. S2. Enlarged view of FTIR analysis for range **(a)** 4000 – 2000 cm^{-1} and **(b)** 2000 – 550 cm^{-1}

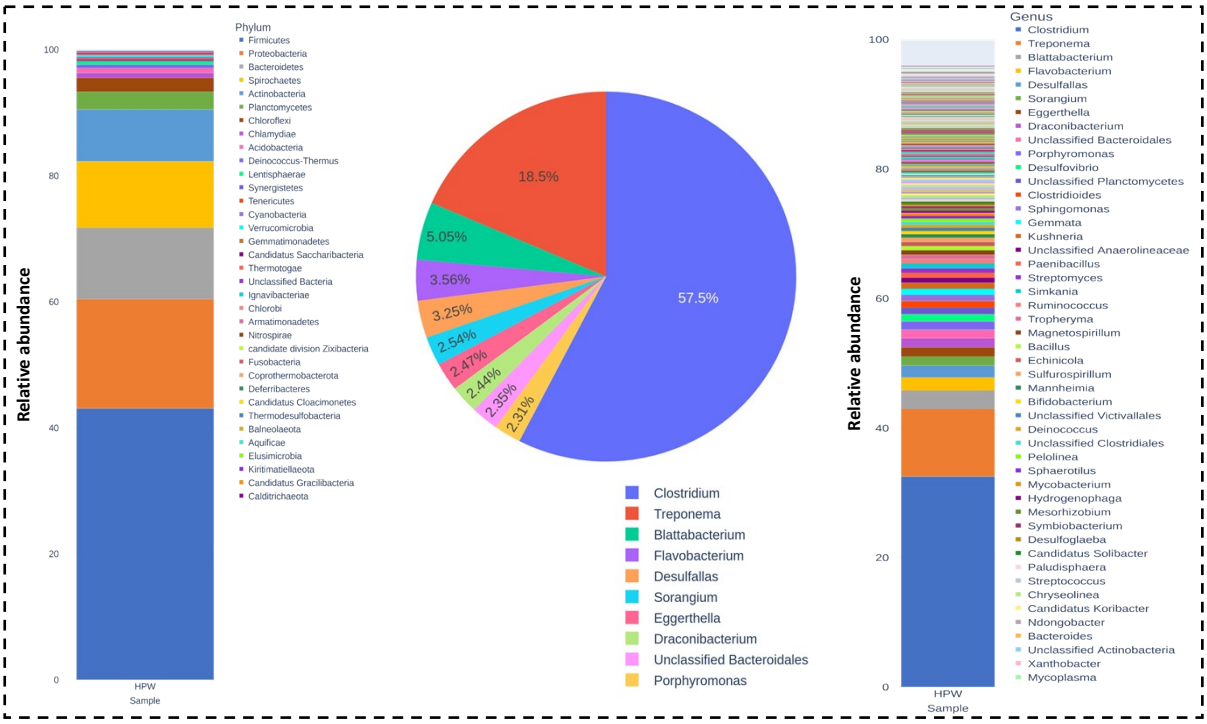

Fig. S3. Metagenomic analysis of microbial culture developed in HTC-PW fed MFC

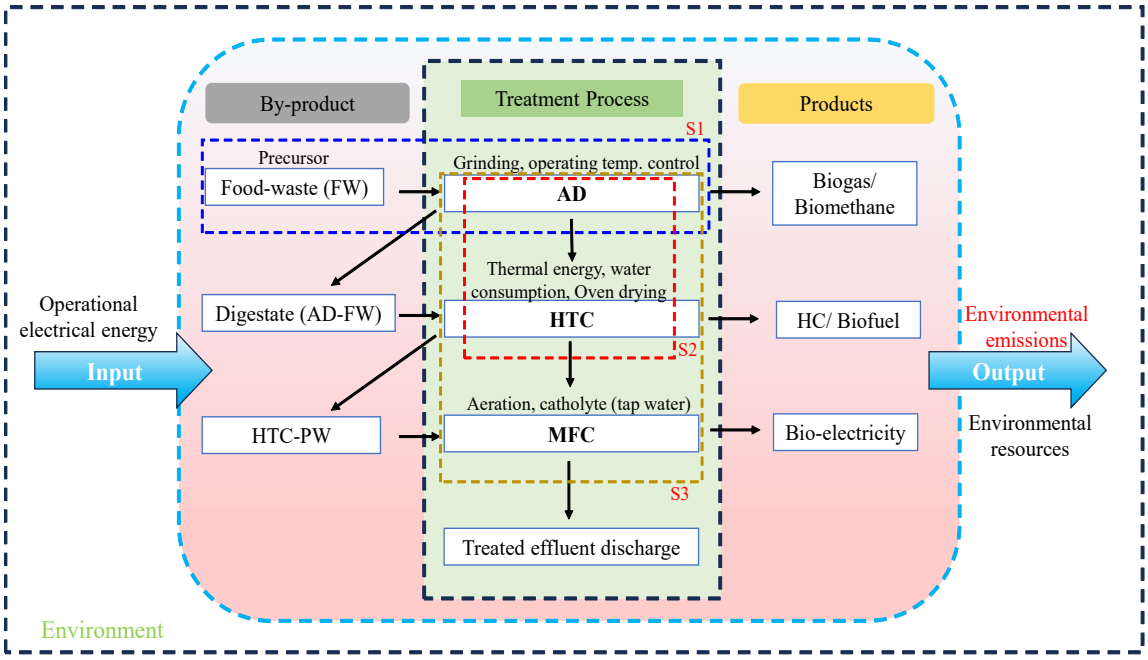

Fig. S4. System boundary for multiple resource recovery via AD, HTC, MFC, and treatment of FW

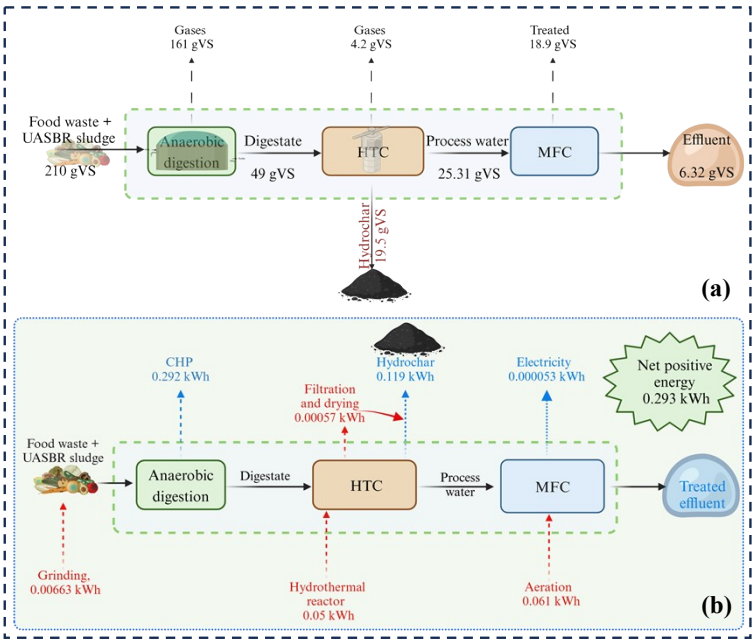

Fig. S5. (a) Mass and (b) energy balance diagram for the integrated treatment scheme AD+HTC+MFC

Table S1. Degradation products of FW-based precursors under hydrothermal carbonization

Target organic component	Degradation compounds and intermediates	Onset HTC Temperature
Hemicellulose	Monomers: Glucose, xylose, and fructose. These smaller compounds can further react through dehydration and fragmentation reactions to form organic acids, furans, and aldehydes. Some of these products might dissolve in the process water, contributing to the chemical composition of the liquid phase, while others can condense and form carbon structures, becoming part of the solid hydrochar.	180 – 200 ℃
Cellulose	Oligomers: Cellohexose, cellopentaose, cellotetraose, cellotriose, cellobiose Cellulose and hemicellulose can be effectively carbonized into spherical hydrochar polymers, consisting of furfural and 5-hydroxymethylfurfural structural units cross-linked with some aromatic structures, together with the aromatic structure of lignin	220 ℃
Lignin	Lignin is extremely resistant and can't be easily breakdown however defragmentation and depolymerization of lignin takes place during HTC. Lignin gets converted to smaller phenolic compounds, such as guaiacol and syringol, as well as other aromatic and aliphatic compounds.	Above 250 ℃

Adapted from the reference [13,14]

Table S2. Role of electro-active communities in the treatment of HTC-PW and power production using MFC

Existing genus	Family/Order	Class	Phylum	Specific role in MFC	References
Clostridium	Clostridiaceae	Clostridia	Firmicutes	Role of converting fermentable substrates (e.g. glucose and propionate) into simple organics	[15]
Treponema (Sp. Caldarium)	Spirochaetales	Spirochaetia	Spirochaetes	Exo-electrogenic activity; Oxidize organic matter Have syntrophic relation with other bacteria in the biofilm	
Blattabacterium	Flavobacteriaceae /Flavobacteriales	Flavobacteriia	Bacteroidetes	In addition to recycling nitrogenous waste, *Blattabacterium* produces amino acids.	[16]
Flavobacterium	Flavobacteriaceae /Flavobacteriales	Flavobacteriia	Bacteroidetes	Digest complex organic molecules (cellulose) and a distinct gliding motility mechanism define the genus Flavobacterium. Distinctive capacity to break down complex plant-derived polysaccharides like glucomannan and pectin, as well as the capacity to secrete several enzymes that are active on carbohydrates through the type IX secretion system unique to Bacteroidetes (T9SS).	[17]
Desulfallas	Desulfallaceae	-	-	Sulphate-reducing bacteria Strictly anaerobes	[18]
Sorangium (sp. Cellulosm)	Polyangiaceae/ Myxococcales	Deltaproteo-bacteria	Proteobacteria	Sorangium and Myxococcus strains are members of the Protobacteria gram-negative delta-subdivision. Cellulose and acetate degraders Responsible for the direct electron transfer to the electrode Remarkable traits shared by members of this taxon include the capacity to develop fruiting bodies, glide on solid surfaces, and build biofilms.	[15,19]
Eggerthella	Eggerthellaceae/ Eggerthellales	Coriobacteriia	Actinobacteria	Capable of oxidation-reduction reactions Resistant to harsh conditions Capable of enhancing bioelectricity production	[20]

Table S3. Life cycle inventory for the treatment of 1 kg of food waste

	Unit	AD	AD+HTC	AD+HTC+MFC
Input				
Electricity for grinding	kWh	0.0063	0.0063	0.0063
Landfilling distance	km	20	nr	nr
Electricity for HTC	kWh	nr	0.05	0.05
Electricity for HTC; filtration	kWh	nr	0.00049595	0.00049595
Electricity for HTC; oven drying	kWh	nr	0.0000763	0.0000763
Water, deionised {RoW}| market for water, deionised | APOS, U	kg	nr	3.3	3.3
Process water from HTC	mL	nr	nr	286
Electricity required for aeration	Wh	nr	nr	0.0612
Output				
Methane	g	1.452	1.484	1.484
Ammonia	g	0.48	0.48	0.48
Dinitrogen monoxide	g	0.03	0.03	0.03
Carbonmonoxide	g	0.15	0.26	0.26
Hydrogen sulfide	g	0.0164	0.0164	0.0164
Sulfurdioxide	g	0.078	0.078	0.078
Nitrogen oxide	g	0.047	0.047	0.047
Non-methane volatile organic compounds	g	0.0062	0.0062	0.0062
effluent COD	g	0.1112	6.9752	2.1704
Digestate as open dump	g	100	100	100
Hydrogen	g	nr	0.0013	nr
Products				
Power recovered from methane through CHP	MJ	1.05	1.05	1.05
Hydrochar	g	nr	30.36	30.36
Power recovered from MFC	Wh	nr	nr	0.053

Note: Inventory was articulated based on the experimental data and assumptions based on literature. [21–24]; nr corresponds to not required.

List of Abbreviations

Anaerobic digestate derived from FW (AD-FW)

Anaerobic digestion (AD)

Biochemical methane potential (BMP)

Burnout temperature (T_b)

Chemical oxygen demand (COD)

Combined heat and power (CHP)

Differential thermogravimetric analysis - differential thermal analysis (DTG-DTA)

Energy densification (ED)

Energy dispersive X-ray (EDX)

Energy recovery efficiency (ERE)

Fixed carbon (FC)

Food waste (FW)

Fourier transform infrared spectroscopy (FTIR)

Fuel ratio (FR)

HC yield (HCY)

High heating value (HHV)

Hydrochar (HC)

Hydrothermal carbonization (HTC)

Ignition temperature (T_i)

Life cycle assessment (LCA)

Life cycle inventory (LCI)

Maximum combustion temperature (T_m)

Microbial fuel cells (MFC)

Process water (PW)

Scanning electron microscopy (SEM)

Up-flow anaerobic sludge blanket reactor (UASBR)

Volatile solids (VS)

X-ray diffraction (XRD)

References

1 S. Panigrahi, H. B. Sharma and B. K. Dubey, *J. Clean. Prod.*, 2020, **243**, 118480.

2 A. M. Buswell and H. F. Mueller, *Ind. Eng. Chem.*, 1952, **44**, 550–552.

3 T. Wang, Y. Zhai, Y. Zhu, X. Gan, L. Zheng, C. Peng, B. Wang, C. Li and G. Zeng, *Bioresour. Technol.*, 2018, **266**, 275–283.

4 A. E871-82, *Standard Test Method for Moisture Analysis of Particulate Wood Fuels 1*, 2014, vol. 82.

5 A. E872 − 82, *Standard Test Method for Volatile Matter in the Analysis of Particulate Wood Fuels*, 2013.

6 A. E 1755 – 01, *Standard Test Method for Ash in Biomass*, 2002.

7 American Public Health Association (APHA), *Standard methods for the examination of water and wastewater standard methods for the examination of water and wastewater*, Washington, 1999.

8 L. P. Xiao, Z. J. Shi, F. Xu and R. C. Sun, *Bioresour. Technol.*, 2012, **118**, 619–623.

9 K. Rathika, S. Kumar and B. R. Yadav, *Sci. Total Environ.*, 2024, **906**, 167828.

10 A. Dhanda, S. M. Sathe, B. K. Dubey and M. M. Ghangrekar, *Sustain. Energy Technol. Assessments*, 2023, **58**, 103378.

11 I. Chakraborty, G. D. Bhowmick, D. Nath, C. N. Khuman, B. K. Dubey and M. M. Ghangrekar, *Int. Biodeterior. Biodegrad.*, 2021, **156**, 105108.

12 S. M. Sathe, I. Chakraborty, V. R. Sankar Cheela, S. Chowdhury, B. K. Dubey and M. M. Ghangrekar, *Bioresour. Technol.*, 2021, **341**, 125850.

13 H. Bhakta Sharma, S. Panigrahi and B. K. Dubey, *Bioresour. Technol.*, 2021, **333**, 125187.

14 C. Zheng, X. Ma, Z. Yao and X. Chen, *Bioresour. Technol.*, 2019, **285**, 121347.

15 Y. Zhang, B. Min, L. Huang and I. Angelidaki, *Bioresour. Technol.*, 2011, **102**, 1166–1173.

16 Z. L. Sabree, S. Kambhampati and N. A. Moran, *Proc. Natl. Acad. Sci. U. S. A.*, 2009, **106**, 19521–19526.

17 J. Kraut-Cohen, O. H. Shapiro, B. Dror and E. Cytryn, *Front. Microbiol.*, 2021, **12**, 1–13.

18 M. Watanabe, M. Fukui and J. Kuever, *Bergey's Man. Syst. Archaea Bact.*, 2020, 1–3.

19 K. Gerth, S. Pradella, O. Perlova, S. Beyer and R. Müller, *J. Biotechnol.*, 2003, **106**, 233–253.

20 K. Sivakumar, H. Ann Suji and L. Kannan, *Mar. Bioenergy Trends Dev.*, 2015, 515–526.

21 P. Roy, A. Dutta and J. Gallant, *Renew. Sustain. Energy Rev.*, 2020, **132**, 110046.

22 A. Mohammadi, G. Venkatesh, M. Sandberg, S. Eskandari, S. Joseph and K. Granström, *Sustain.*, 2020, **12**, 1–15.

23 C. Huang, B. A. Mohamed and L. Y. Li, *Chem. Eng. J.*, 2023, **457**, 141284.

24 Y. Yang, X. Li, X. Yang and Z. He, *RSC Adv.*, 2016, **6**, 49787–49791.